7th International Symposium on Superalloy 718 and Derivatives
Edited by: E.A. Ott, J.R. Groh, A. Banik, I. Dempster, T.P. Gabb, R. Helmink, X. Liu, A. Mitchell, G.P. Sjöberg, and A. Wusatowska-Sarnek
TMS (The Minerals, Metals & Materials Society), 2010

EFFECT OF MICROSTUCTURE AND ENVIRONMENT ON THE HIGH-TEMPERATURE OXIDATION BEHAVIOR OF ALLOY 718PLUS

Kinga A. Unocic[1], Raymond R. Unocic[1], Bruce A. Pint[1] and Robert W. Hayes[2]

[1]Oak Ridge National Laboratory, Oak Ridge, TN 37831
[2]Metals Technology Inc. Northridge, CA 91324
Keywords: 718Plus, high-temperature oxidation, Cr_2O_3, δ-phase

Abstract

The effect of microstructure on the oxidation behavior of 718Plus was evaluated in dry air, wet air and steam environments at 650°-700°C. Tests at 800°C were also performed in an attempt to accelerate the testing. Oxidation in wet air simulates turbine combustion environments and causes net mass losses at 650°-700°C because of the volatilization of Cr oxy-hydroxides that is not observed in ambient air testing. At 800°C, mass gains were measured but significant Cr depletion can be measured in the alloy after exposure due to volatilization. Changes in temperature and environment had much larger effects on oxidation performance than the two microstructures evaluated. Advanced characterization techniques were used to compare the differences in the oxide scale formed on alloys with different process conditions. At higher temperatures, the surface oxide was primarily identified as Cr_2O_3 by x-ray diffraction. Cross-section analysis showed an increase in internal oxidation attack with increasing temperature. The internal attack appeared to be associated with rod-shaped Ni_3Nb precipitates (δ-phase). Because of the changes in microstructure at 800°C, the steam and wet air evaluations appeared to be less relevant to lower temperatures. Thus, increasing the exposure temperature to 800°C does not appear to be a good strategy for accelerated testing of 718Plus.

Introduction

Alloy 718 is widely used for high temperature components in power generation and aircraft turbines [1-3]. The service life is expected to be many thousands of hours (at least 30kh) while maintaining a stable structure. In order to increase the maximum operating temperature (650°C) and performance, alloy 718Plus was developed for improved thermal stability. Alloy 718Plus includes significant composition changes from 718: Fe content was reduced and 10% Co was added as well as an increase in Al content to 1%. The higher Al content promotes the formation of the $L1_2$ γ′ phase ($Ni_3(Al,Ti)$), which has higher thermal stability than DO_{22} γ′′ phase (Ni_3Nb) [4-8]. The growth rate of γ′ in 718Plus is much slower than the γ′′ phase in 718, which results in slower associated formation of the stable orthorhombic δ phase (Ni_3Nb). Also, the addition of 1% W further increases the high temperature strength. The compositions are summarized in Table I.

One of the main environmental issues that has been studied on 718 is the environmental effect on crack growth. Many superalloys are susceptible to environmentally enhanced intergranular cracking in the presence of oxygen, water vapor, sulphur, and chlorine [**2**]. Typically, oxidation is sensitive to the oxygen partial pressure, which will determine which phases are thermodynamically stable. In ambient air at temperatures near 650°C, 718 will form a transient (i.e. initial) oxide rich in Fe and Ni, likely a spinel-type $Ni(Fe,Cr)_2O_4$ oxide, followed by the formation of an underlying Cr-rich layer, typically Cr_2O_3, which is more thermodynamically

stable [9-11]. The long-term oxidation rate is controlled by growth and transport through this external Cr-rich oxide layer or scale. At lower oxygen partial pressures, Fe- and Ni-rich oxides may not be stable and the scale is primarily Cr-rich oxide. At higher temperatures, other spinel-type oxides have been observed; $NiCr_2O_4$ and $NiFe_{2-x}Cr_xO_4$ [12]. Also, Nb-containing oxides and carbides can form during oxidation at very high temperatures [3].

Relatively little attention has been given to the effect of water vapor on the oxidation of superalloys like 718. Water vapor is present in combustion environments but its affect is not always considered. All Fe- and Ni-base chromia-forming alloys are affected by the reaction of the scale with O_2 and H_2O to form a volatile oxy-hydroxide [13, 14]:

$$Cr_2O_{3(s)} + O_{2(g)} + H_2O_{(g)} = CrO_2(OH)_{2(g)} \quad (1)$$

Since the volatilization can follow linear kinetics, the longer-term loss of Cr from the substrate is significantly higher than in environments that do not contain water vapor. However, steam environments with low dissolved oxygen do not experience this volatilization [15]. Some studies have examined the effect of wet air environments on 718Plus, including evidence of grain boundary cracking of fully recrystallized 718Plus [16]. It was concluded that high-angle grain boundaries were the preferred sites for oxygen penetration. Additionally, the presence of δ phase oriented along grain boundaries provided the path for oxygen penetration and subsequent embrittlement.

The aim of the current study is to examine the effect of two different microstructures (worked and recrystallized) on the high temperature oxidation behavior of 718Plus in laboratory (dry) air and wet (10 vol.% H_2O) air and examine the effect of accelerated testing at high temperature (800°C).

Experimental Procedure

Alloy 718Plus with a composition shown in Table I was received in the as-forged condition. The alloy subsequently underwent two different heat treatments with details presented in Table II. The first heat treatment is a standard (Std) heat treatment, which is employed in the industry and results in a worked microstructure.

Table I. Chemical composition of 718Plus is determined by ICP and combustion methods (in wt.% except S in ppmw)

Alloy	Ni	Cr	Mo	W	Co	Fe	Nb	Ti	Al	Mn	C	S	P
718	54.1	18.0	3.1	0.02	0.3	17.6	5.0	1.0	0.5	0.1	0.04	<10	0.01
718Plus	52.5	17.9	2.67	0.98	8.9	9.5	5.3	0.8	1.3	0.04	-	-	0.002

In order to study the effect of grain size on high temperature oxidation, the second heat treatment (Rx+Std) incorporates an additional heat treatment above the δ solvus (1038°C/1h) prior to the standard treatment. As a consequence the microstructure was fully recrystallized prior to the standard treatment. For metallographic examination of the grain size, samples were polished using standard techniques followed by etching with modified Kalling's (100 ml HCl, 100 ml methanol, 15g $CuCl_2$) etchant.

Table II. Heat treatment applied to 718Plus

Name	Heat Treatment	Grain Size (μm)
Standard (Std)	968°C (1775F) 2 hours / oil quench 788°C (1450F) 8 hours / air cooled 704°C (1300F) 8 hours / air cooled	63
Recrystallized (Rx+Std)	1038°C (1900F) 1 hour / air cooled 968°C (1775F) 2 hours / oil quench 788°C (1450F) 8 hours / air cooled 704°C (1300F) 8 hours / air cooled	100

High temperature oxidation studies were performed in laboratory air (dry air) and in air + 10 vol.% water vapor (wet air) at 650°C, 700°C, and 800°C. The 800°C temperature is higher than the typical operating temperature for 718 or 718Plus and was selected to accelerate the oxidation testing in an attempt to simulate to the long service life of these materials at lower temperatures. The wet air environment was generated in an alumina tube furnace by atomizing water into the flowing air stream and calibrating the amount of injected water with the air flow rate.

Oxidation coupons (1.5 x 10 x 19 mm) were polished to 600 grit for the wet air experiments and to 0.3 μm alumina for the air experiments. All samples were ultrasonically cleaned in acetone and methanol prior to oxidation testing. One set of specimens was removed at 1kh for characterization. A second set will continue for longer-term evaluations.

After exposure, coupons were examined in plan-view and then Cu-plated, sectioned, and polished for metallographic analysis. Characterization included light microscopy (LM), x-ray diffraction (XRD), scanning electron microscopy (SEM) using a Hitachi S4800, and electron probe microanalysis (EPMA) using a JEOL 8200 with wavelength dispersive x-ray analysis.

Results

Alloy microstructure

Figure 1 shows polished cross-sections of the two different heat treatments of 718Plus. Standard heat treatment (Std) resulted in a lightly worked structure with an average grain size of 63 μm (standard deviation of 38 μm) (ASTM 4.5) (Fig. 1a). The structure after the Rx+Std treatment was more uniform (Fig. 1b) and had an average grain size of 100 μm (standard deviation of 55) (ASTM 3.5).

Effect of water vapor on oxidation

Figures 2-5 compare the oxidation behavior of 718Plus tested in laboratory air and wet air at 650°-800°C. At 650°C, the specimens with the two microstructures exhibited small mass gains in laboratory air and a small mass loss in wet air, Figure 2. In general, the net measured mass change, ΔM_{total}, of an oxidation specimen can be described by the following equation:

$$\Delta M_{total} = \Delta M_{oxide} - \Delta M_{spall} - \Delta M_{volatile} \quad (2)$$

where ΔM_{oxide} is the mass gain due to oxide scale formation, ΔM_{spall} and $\Delta M_{volatile}$ are the mass losses due to scale spallation and volatilization (i.e. Eqn. 1), respectively. Since no scale

spallation was observed at 650°C on the surface of the smaples after analysis via SEM, the low mass change at 650°C in wet air is attributed to volatilization in the presence of water vapor.

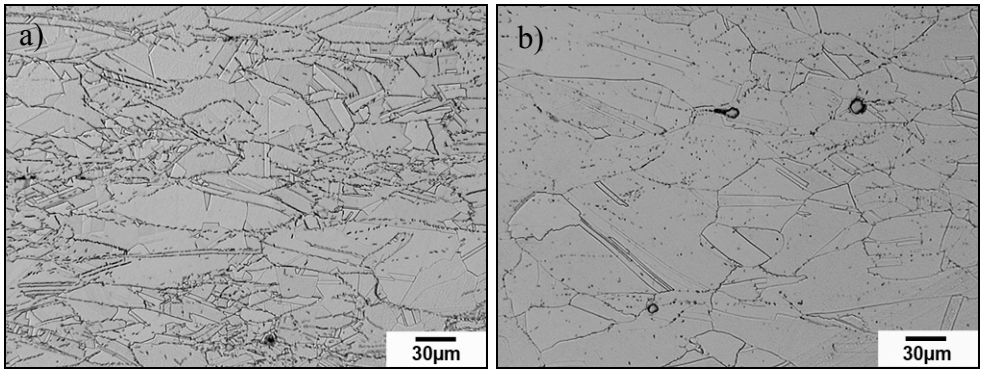

Figure 1. Optical images representing the microstructure after a) standard (Std) and b) recrystallized (Rx+Std) heat treatment.

At 700°C, small but significantly different mass gains were measured in laboratory air and a consistent mass loss was measured in the presence of water vapor, Figure 3. Again, this difference is attributed to the volatilization of the Cr oxy-hydroxide. At 600°C and 700°C, both 718Plus microstructures performed very similarly in wet air. Differences in mass gains were observed in laboratory air at both temperatures; however, longer-term results are needed, along with characterization of the reaction products, to evaluate these differences. In these initial results, the mass gain was significantly lower at 700°C for the larger grain size.

At 800°C, the mass changes in laboratory and wet air were more similar for the first 1kh, Figure 4. Two specimens are shown for each condition, one that was removed after 1kh for characterization and a second specimen that is continuing for exposure to ~5kh. At longer times (>2.2kh), the specimens in wet air appear to begin losing mass. Considering Eqn. 2, the mass gain due to oxide growth appears to dominate the mass change at 800°C, compared to the lower temperatures. There appears to be little difference in performance due to microstructure at this temperature, although the smaller grain size showed a slightly higher mass gain in both environments.

Figure 5 summarizes the mass change for 718Plus with the standard heat treatment after 1kh at the three temperatures in laboratory air and wet air. At each temperature, the mass gain in air is higher than in wet air and this difference is attributed to the volatilization of the Cr oxy-hydroxide. At 650° and 700°C, where the oxide scale is thin, there is a net mass loss in wet air. At 800°C where the oxide is much thicker, there is a net mass gain in wet air.

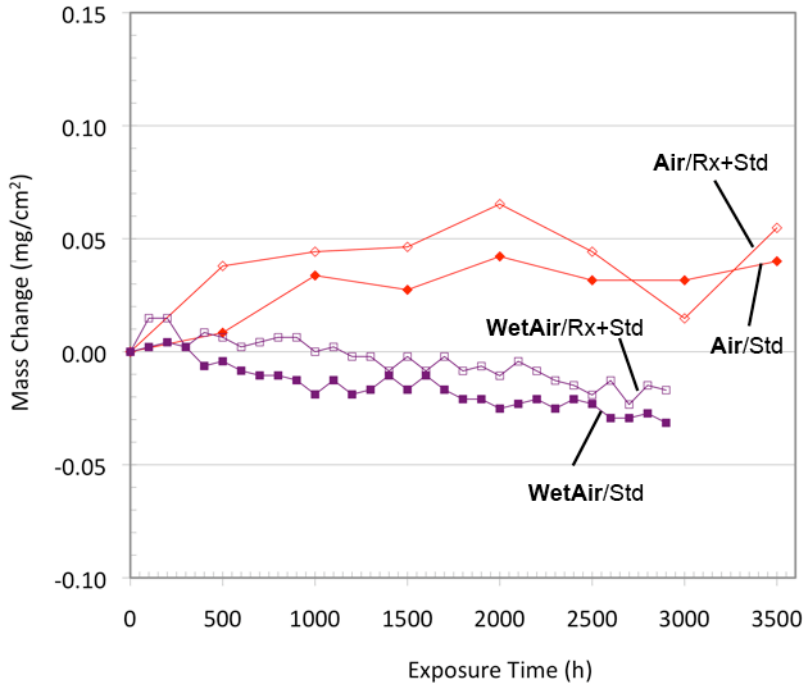

Figure 2. Effect of environment and microstructure on mass change data after exposure of 718Plus to *air* and *wet air (air +10% water vapor)* at 650°C.

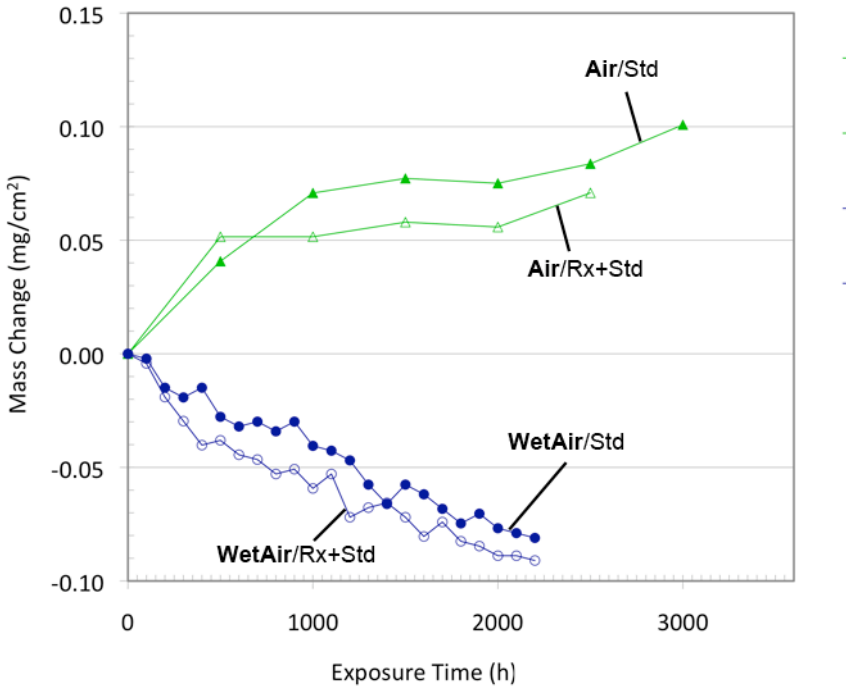

Figure 3. Effect of environment and microstructure on mass change data after exposure of 718Plus to *air* and *wet air (air +10% water vapor)* at 700°C.

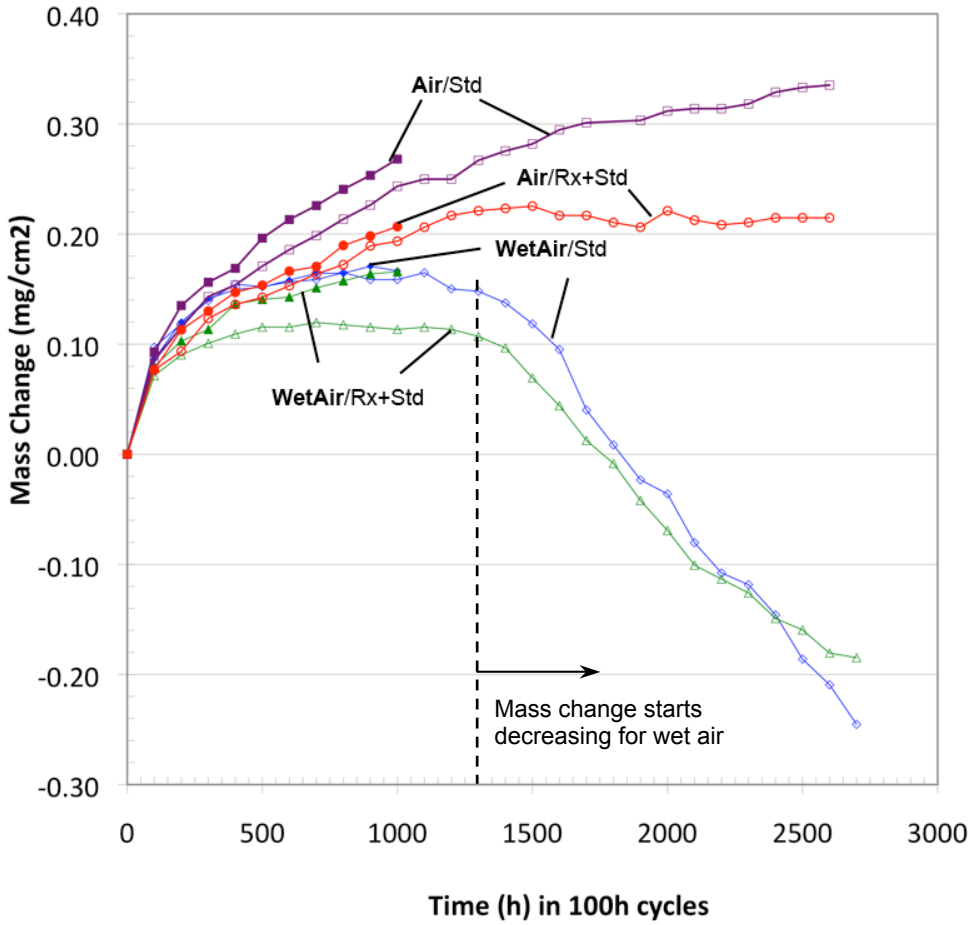

Figure. 4 Effect of environment (air vs. wet air) and microstructure (deformed (Std) vs. recrystallized (Rx+Std)) after exposure at 800°C.

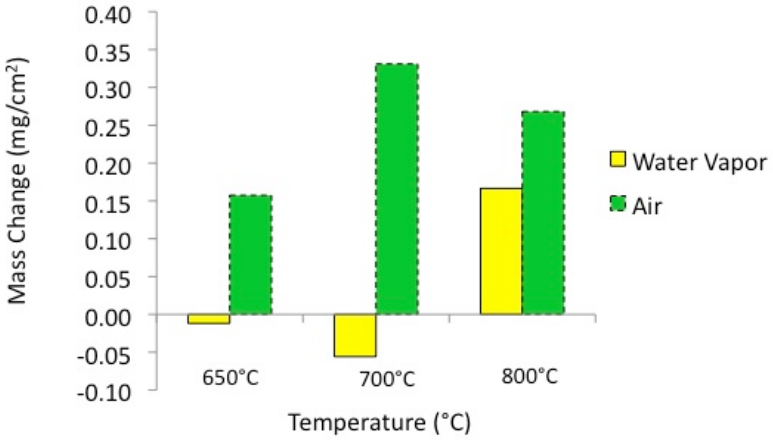

Figure 5. Mass change data for Std 718Plus obtained after 1kh in air and wet air at 650°C, 700°C, and 800°C.

Figure 6 shows some initial results of the 718Plus specimens in 17bar steam at 800°C. In steam, formation of the oxy-hydroxide does not occur because of the lack of free O_2 in the environment. Thus, no mass loss was expected. The mass gains in steam are significantly higher than the mass gains in laboratory air or wet air suggesting a much faster rate of attack.

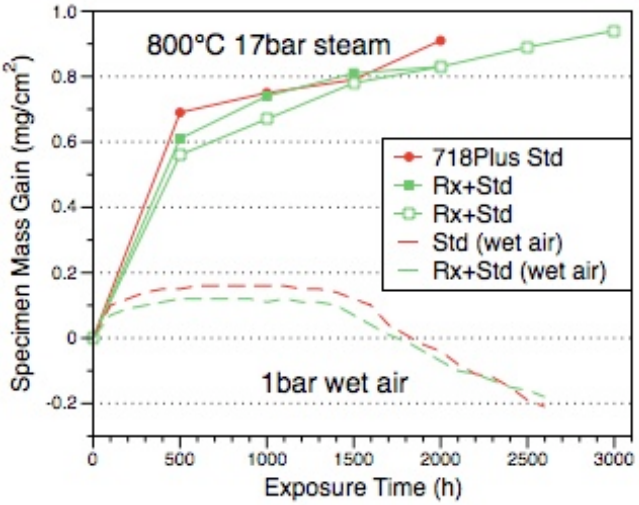

Figure 6. Mass change of 718Plus specimens in 500h cycles at 800°C in 17bar steam compared to wet air.

Scale characterization

Figure 7 shows the gas-interface scale morphology formed on 718Plus (Std) after 1kh in wet air at the three oxidation temperatures. There was no difference in scale morphology for the two 718Plus microstructures. As mentioned earlier, there was no spallation observed under any of these conditions. The high magnifications in Figures 7a and 7b emphasize the fine grains formed in the surface scale at 650° and 700°C, respectively. X-ray diffraction showed very small Cr_2O_3 peaks at 650°C consistent with the low mass gain at this temperature, Figure 2. More distinctive Cr_2O_3 X-ray peaks were observed at the higher temperatures. Larger oxide grains and more transient oxides were observed after oxidation at 800°C, Figure 7c and 7d.

Figure 8 compares the gas-interface scale morphology formed on both 718Plus microstructures after 1kh at 800°C in laboratory air. At lower magnification, Figures 8a and 8c, the grain boundaries appear to be visible with a thinner oxide. At higher magnification, Figures 8b and 8d, large crystals are observed at the scale/gas interface, with a higher density on the finer grained (Std) microstructure.

Figure 9 shows polished cross-sections of the specimens exposed for 1kh. The specimens from 650° and 700°C (Figs. 9a-9d) are at a higher magnification because of the thinner reaction products. Very little internal attack was observed at 650°C; however, large δ -precipitates (Ni_3Nb) were present in the Std heat treated specimen (Fig. 9a). At 700°C, a thin (<1μm) surface oxide also was formed but significant internal attack was observed, Figures 9c and 9d. The internal attack sometimes appeared to follow the Ni_3Nb/matrix interfaces. At 800°C, the surface scale was significantly thicker (~2μm) with a slightly thicker scale forming in wet air (Figures 9e and 9f) compared to laboratory air (Figures 9g and 9h). As at 700°C, the internal attack appeared to follow the Ni_3Nb/matrix interfaces. Wet air also gave a significant increase in

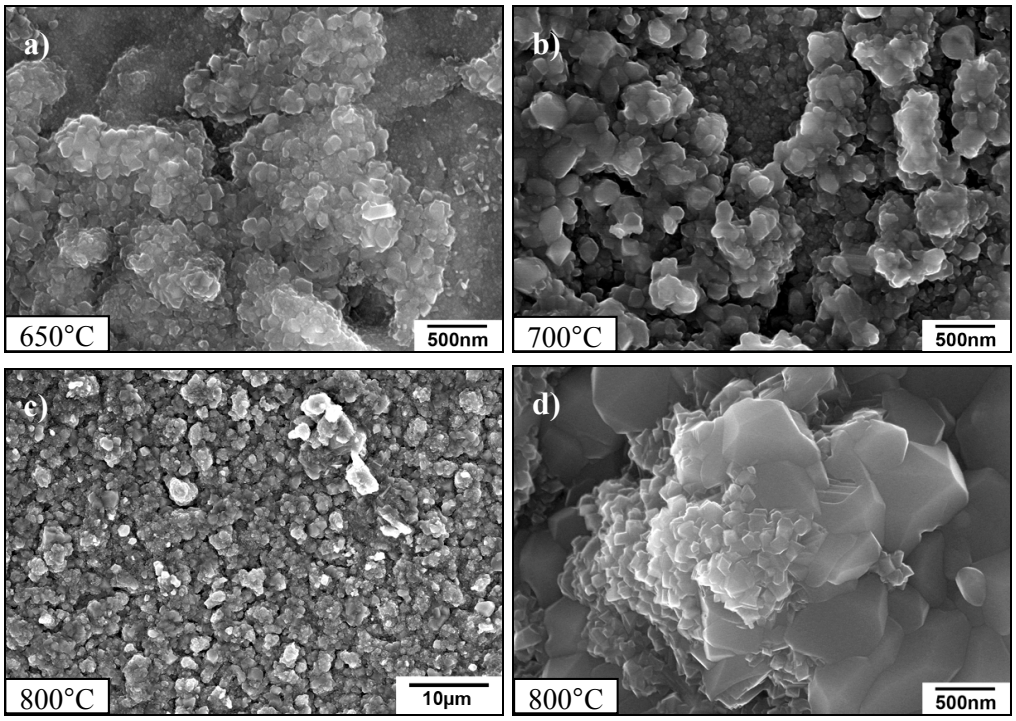

Figure 7. Secondary electron plan-view images of the scale formed after 1kh in wet air at a) 650°C, b) 700°C, c) 800°C and d) 800°C - higher magnification image.

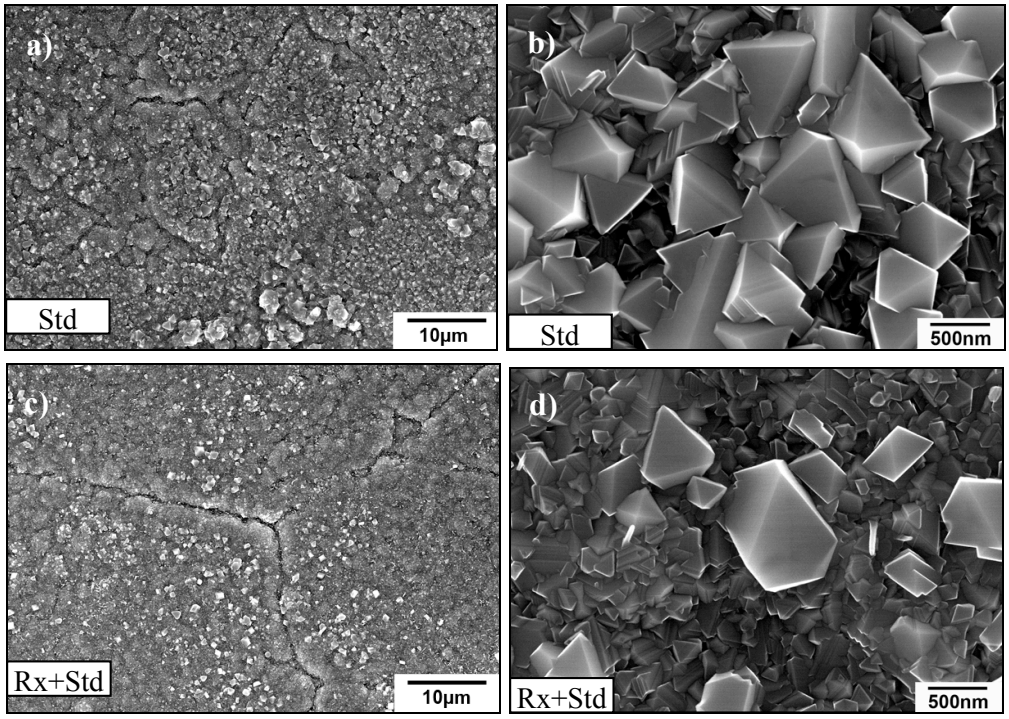

Figure 8. Secondary electron images of the top surface of alloy 718Plus after exposure to air for 1kh at 800°C for microstructure with a-b) smaller grains (Std), and c-d) larger grains (Rx+Std).

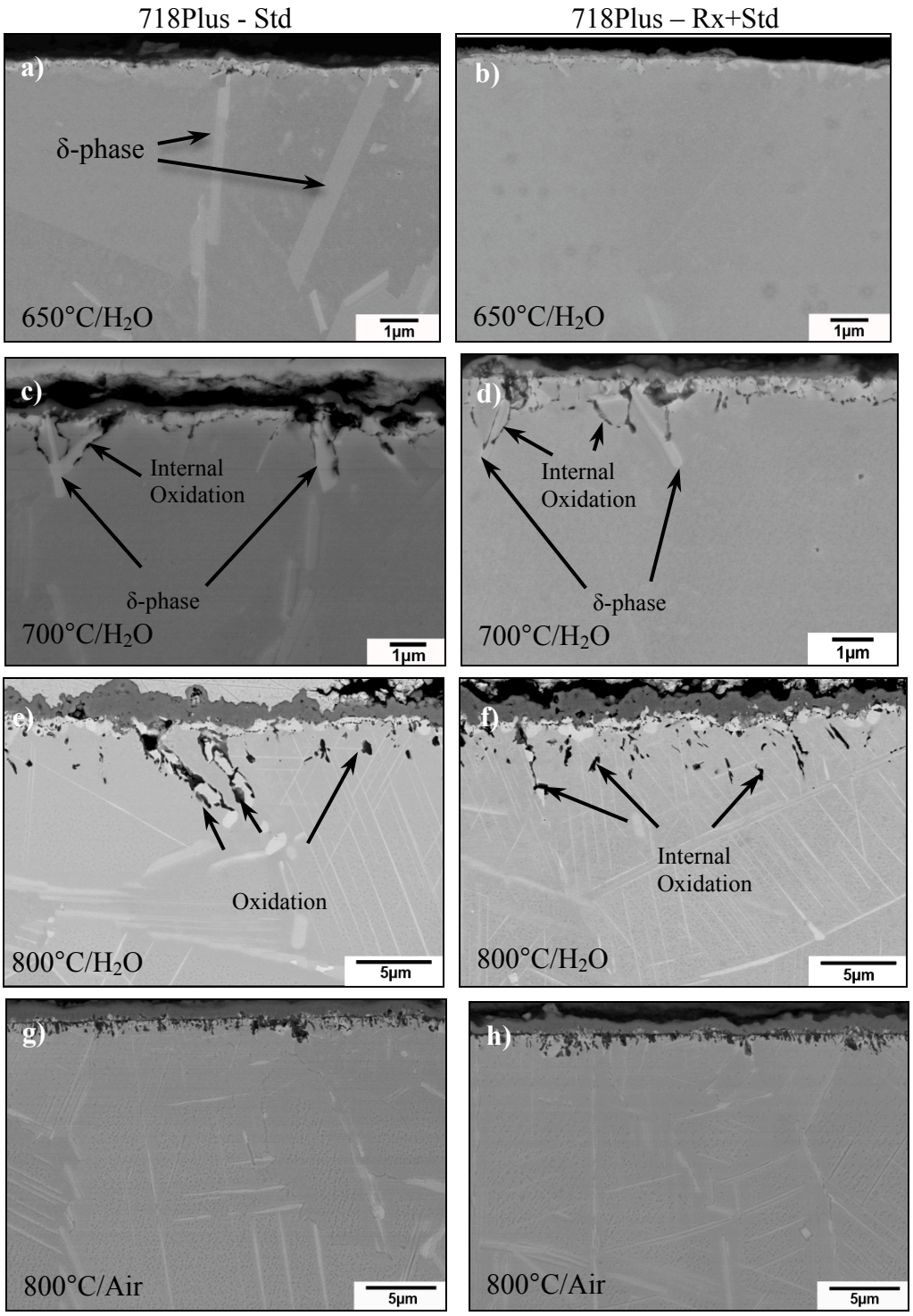

Figure 9. SE images of the cross-sections after exposure of 718Plus for 1kh at a) 650°C/wet air/Std, b) 650°C/wet air/Rx+Std, c) 700°C/wet air/Std, d) 700°C/Rx+Std, e) 800°C/wet air/Std, f) 800°C/wet air/Rx+Std, g) 800°C/air/Std, h) 800°C/air/Rx+Std.

the depth of internal attack. The amount of internal attack in wet air appeared higher in the Std heat treatment, although the depth was similar, Figures 9e and 9f. This difference is in agreement with the mass change data in Figure 4. The standard heat-treatment was reported to result in a more uniformly distributed δ-phase in 718Plus [16], however, that is not necessarily reflected in the images in Figure 9. Exposure at 800°C appeared to result in γ′ coarsening (100-150nm) and a higher density of δ-phase which is detrimental to 718Plus oxidation resistance.

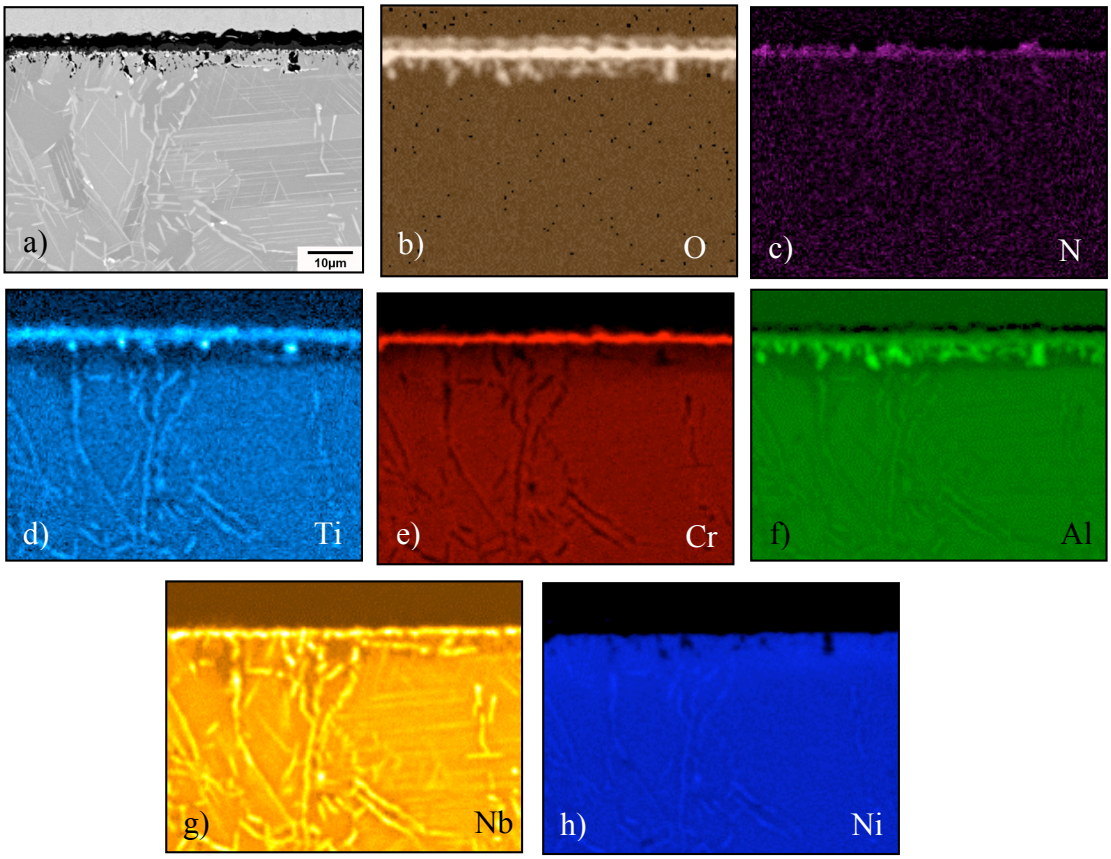

Figure 10. Cross-section of the 718Plus (Std) after 1kh at 800°C (a) secondary electron image and EPMA elemental maps (b) O, (c) N, (d) Ti, (e) Cr, (f) Al, (g) Nb and (h) Ni.

Figure 10 shows EPMA x-ray maps of the scale formed on 718Plus (Std) after 1kh at 800°C in wet air. The maps appear to show a multi-layer oxide scale with a Ti-rich outer layer and a Cr-rich inner layer. There may be some N enrichment. The internal oxide appears to be primarily Al_2O_3, as expected. The Nb elemental map clearly shows the δ-phase precipitates and a concentration of Nb near the metal-scale interface, perhaps rejected from the oxidation front.

Figure 11 shows cross-sections of the 718Plus specimens exposed in 17bar steam for 2kh at 800°C. The attack is similar as that observed in wet air at 800°C atmospheric pressure. Because of the lack of free oxygen in the steam environment, formation of Cr oxy-hydroxide is not expected [**15**], and Cr depletion has not been observed in a chromia-forming steel [17].

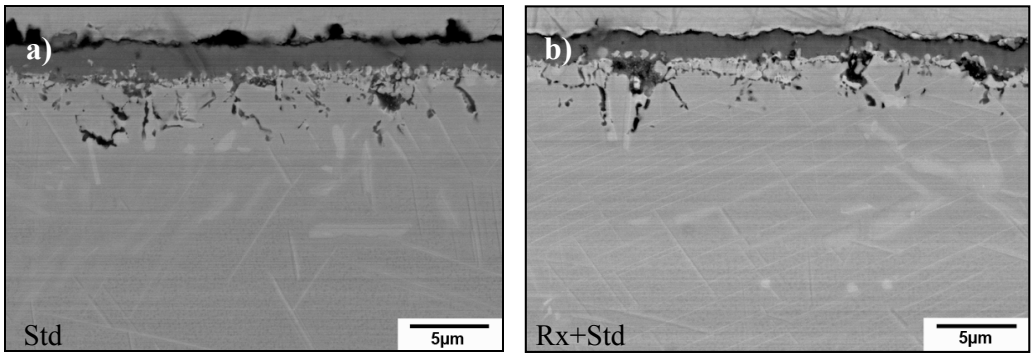

Figure 11. SE images of polished sections of 718Plus exposed for 2kh at 800°C in 17bar steam for samples with a) smaller grains (Std) and b) larger grains (Rx+Std).

Alloy Characterization

In order to further study the effect of water vapor on Cr depletion in the substrate, EPMA line composition profiles were performed on the cross-section of the specimens exposed for 1kh at the three temperatures. The beginning of the EPMA lines was at the top surface of the specimens. Figure 12 compares profiles after exposure at 800°C in wet and laboratory air for the two different microstructures. In the profile, the metal-oxide interface has been set to zero so the distance values less than zero reflect the external scale that has a high Cr content, while the distance values greater than zero reflect the alloy. Therefore, beneath the scale, the Cr depletion is observed in laboratory and wet air for both microstructures. Also, the finer grained (Std) microstructure resulted in greater surface depletion (<8wt%Cr) and depletion to a greater depth than the recrystallized microstructure (Fig. 12). In laboratory air, less Cr depletion was observed as Cr was not lost due to volatilization of $CrO_2(OH)_2$ and the scale formed was not as thick as that formed in wet air (Fig. 9).

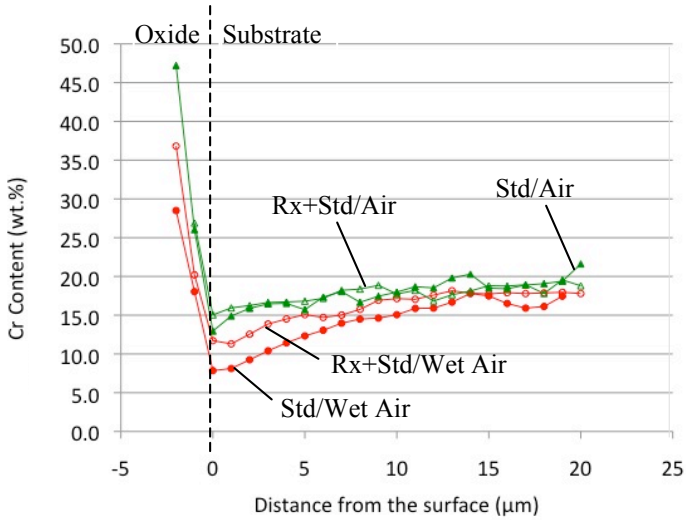

Figure 12. Cr content by EPMA as a function of distance from the surface acquired from the sample cross-sections for 718Plus after exposure for 1kh at 800°C in air and wet air for two different microstructures.

Figure 13a compares the Cr line profiles in the standard 718Plus specimens as a function of temperature after 1kh in wet air. As expected, the Cr depletion increased significantly with temperature as the scale thickness increased and the amount of volatilization also is expected to increase with exposure temperature. Figure 13b shows Al line profiles from the same specimens in Figure 13a. There is a slight enrichment of Al in the scale but very little depletion at 650° and 700°C. At 800°C, there is Al enriched in oxides near the surface and a significant Al depletion in the adjacent metal. This depletion is typical of internal oxidation [18].

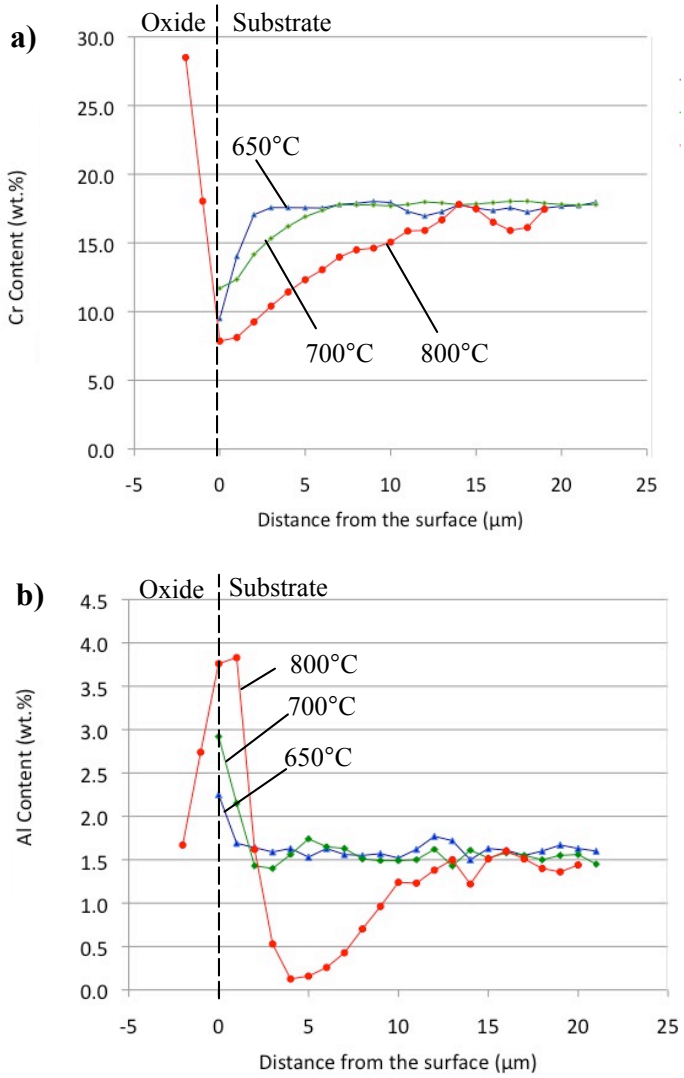

Figure 13. a) Cr and b) Al content by EPMA as a function of distance from the surface acquired from the sample cross-sections for 718Plus after 1kh high-temperature oxidation.

Discussion

Many 718Plus oxidation studies involve short times and/or higher temperatures. The current study has initially characterized oxidation after 1kh, but longer-term (5kh) exposures are being conducted to confirm these observations at longer times. Because of the long lifetimes expected for 718Plus components, one strategy to accelerate the oxidation testing is to increase the exposure temperature. In this study, 800°C was used for accelerated testing, resulting in a much

thicker surface oxide than was formed at 650° or 700°C. However, there was evidence of microstructural changes for 718Plus after oxidation at this temperature. Due to the complex phase composition, thermal stability is more of an issue with this material than alloys with simpler compositions. Therefore, this acceleration strategy is questionable. Also, the temperature dependence of the competing oxide growth and oxy-hydroxide volatilization are not the same. Therefore, the effect of water vapor may be different at 800°C compared to more typical service temperatures.

Oxidation studies in water vapor may be more representative of other service combustion environments such as in gas turbines. Crack growth studies have been conducted in wet air environments and long-term studies will quantify the depth of material affected by this environment. From the 1kh results, it is apparent that 718Plus is affected at a greater depth in the presence of water vapor. One problem with testing in water vapor is that the mass gain measured is more difficult to extrapolate to longer times. For oxidation in air, parabolic kinetics for the mass gain and scale thickness readily lead to long-term predictions. In wet-air, para-linear kinetics are expected due to the combination of oxide growth and volatilization. However, the volatilization is dependent on the water vapor content and gas velocity [15]. Therefore, data from laboratory experiments with a relatively low gas velocity (~1.5cm/s) will not provide accurate rate data for applications in turbines or other high velocity environments.

There was not a strong effect of 718Plus microstructure on oxidation behavior in these initial observations. Perhaps longer exposures will cause the two microstructures to differentiate further. Generally, finer-grained alloys tend to form less transient oxide and more easily form a protective scale because there are more short circuit diffusion paths in the alloy for Cr transport to the oxidation front. However, the coarse-grained structure (Rx+Std) often had smaller mass gains and less reaction product. It appeared that there was less δ phase present near the surface, only at the grain boundaries, of the Rx+Std material, which resulted in less internal oxidation. After oxidation at 800°C, the microstructures appear more similar so the difference in performance may be reduced with longer exposures. Characterization of the longer-term (5kh) specimens at 650° and 700°C will provide more information about the effect of microstructure on the oxidation behavior.

Conclusions

Specimens of 718Plus with two different microstructures, with and without recrystallization, were evaluated at 650°-800°C. The comparison between laboratory air and wet air illustrated the role of water vapor in accelerating the oxidation attack, especially increasing the amount of internal oxidation and Cr depletion from the near-surface region. Because of the volatilization of the Cr oxy-hydroxide, mass losses were measured after 1kh at 650° and 700°C. Relatively thin, Cr-rich external oxide scales formed at these temperatures. Attempting to accelerate the oxidation test by increasing the oxidation temperature to 800°C produced questionable results because the microstructure coarsened and there was an increase in the rod-shaped δ (Ni_3Nb) phase in the alloy. Internal oxidation increased with exposure temperature and for the most part appeared to follow the δ-matrix interfaces. In general, only minor changes were noted in the oxidation behavior because of the microstructure. The expected benefit of a finer alloy grain size was not evident. The standard heat treatment (Std) resulted in slightly higher mass gains and internal attack because of a higher fraction of δ phase at the specimen surface compared to the recrystallized microstructure (Rx+Std).

Acknowledgements

The authors are grateful to H. Longmire, T. Brummett, G. Garner, and L. Walker for assistance with the experimental work. This research was sponsored by the U.S. Department of Energy and Office of Coal and Power R&D.

References

1. J.F. Radavich, "Long Time Stability of a Wrought Alloy 718 disk," *Superalloy 718 - Metallurgy and Applications* (1989), 257-268.
2. D.A. Woodford, "Gas Phase Embrittlement and Time Dependent Cracking of Nickel Based Superalloys," *Energy Materials*, 1 (2006), 59-79.
3. L. Geng, Y.S. Na and N.K. Park, "Oxidation behavior of alloy 718 at high temperature," *Materials and Design*, 28 (2007), 978-981.
4. H.F. Merrick, "Precipitation in Nickel-base Alloys," *Precipitation Process in Solids* K.C. Russel and H.I. Aaronson, eds., the TMS-AIME, Warrendale, PA (1978), 161-190.
5. M. Sundararaman, P. Mukhopadhyay and S. Banerjee, "Precipitation of the δ-Ni_3Nb Phase in Two Nickel-Base Superalloys," *Metallurgical Transactions A*, 19A (1988), 453-465.
6. M. Sundararaman, P. Mukhopadhyay, S. Banerjee, "Some Aspects of the Precipitation of Metastable Intermetallic Phases in Inconel 718," *Metallurgical Transactions A,* 23A (1992), 2015-2028.
7. J.P. Collier, S.H. Wong, J.C. Phillips and J.K. Tien, "The Effect of Varying Al, Ti, and Nb Content on the Phase Stability of Inconel 718," *Metallurgical Transactions A*, 19A (1988), 1657-1666.
8. J.P. Collier, A.O. Selius and J.K. Tien, "On Developing a Microstructurally and Thermally Stable Iron-Nickel Base Superalloy," *Superalloys* (1988), 43-52.
9. E. Andrieu, R. Molins, H. Ghonem and A. Pineau, "Intergranular Crack Tip Oxidation Mechanism in a Nickel-based Superalloy," *Materials Science and Engineering*, A154 (1992), 21-28.
10. R. Molins and E. Andrieu, "Analytical TEM Study of the Oxidation of the Nickel Based Superalloys," *Journal de Physique* IV 3 (1993), 469-475.
11. E. Andrieu, R. Cozar and A. Pineau, "Effect of Environment and Microstructure on the High Temperature Behavior of Alloy 718," *Superalloy 718 - Metallurgy and Applications* (1989), 241-256.
12. M. Lenglet, R. Guillamet, J. Lopitaux and B. Hanoyer, "Initial Stages of Oxidation of Inconel 718 by FTIR spectroscopy," Materials Research Bulletin 25 (6) (1990), 715-722.
13. H. Asteman, J.E. Svensson, M. Norell and L.G. Johansson, "Influence of Water Vapor and Flow Rate on the High-Temperature Oxidation of 304L; Effect of Chromium Oxide Hydroxide Evaporation," *Oxidation of Metals*, 54 (2000), 11-26.
14. E.J. Opila, "Volatility of Common Protective Oxides in High-Temperature Water Vapor: Current Understanding and Unanswered Questions," *Materials Science Forum*, 461-464 (2004), 765-774.
15. D.J. Young and B.A. Pint, "Chromium Volatilization Rates from Cr_2O_3 Scales into Flowing Gases Containing Water Vapor," *Oxidation of Metals*, 66 (2006), 137-153.
16. K.A. Unocic, R.W. Hayes, M.J. Mills and G.S. Daehn, "Microstructural Features Leading to Enhanced Resistance to Grain Boundary Creep Cracking in Allvac 718Plus," *Metallurgical and Materials Trans. A*, 41A (2) (2010), 409-420.
17. B.A. Pint, J. Haynes, Y. Zhang, K. More and I. Wright, "The Effect of Water Vapor on the

Oxidation Behavior of Ni-Pt-Al Coatings and Alloys," *Surface & Coatings Technology*, 201 (2006), 3852.
18. D.L. Douglass, "A Critique of Internal Oxidation in Alloys During the Post-Wagner Era," *Oxidation of Metals*, 44 (1995), 81-111.